LAB-TO-LAB VARIATION IN TESTING FANS

Mark STEVENS[1], Marton GYURO[2]

[1] *AMCA International, 30 West University Drive, Arlington Heights, Illinois 60004, USA*

[2] *Greenheck Fan Corporation, 1100 Greenheck Drive, Schofield, WI 54476, USA*

SUMMARY

AMCA International conducted a round robin series of test on three fans to investigate lab-to-lab variation in air performance and sound test results. The purpose of the round robin was to advance the science of testing fans in accordance with ISO and AMCA standards, specifically ISO 5801, ISO 13347, AMCA 210 and AMCA 300, and to advance our knowledge of test result uncertainty such that tolerances for certification programs and acceptance tests are fair and realistic.

INTRODUCTION

Three fans were part of the round robin, and all three were tested on multi-nozzle chambers. Centrifugal and tubeaxial fans were tested using a chamber at the fan's outlet, and both were powered by dynamometer. A vaneaxial fan was tested on a chamber at the fan's inlet and was powered by a calibrated motor. All participating labs used the same motor calibration. All three fans were sound tested in a reverberant room.

What we found is that the agreement between labs is actually very good. The determination of air power, power consumption and sound power through the measurement of pressure, temperature, torque, rotational speed and sound pressure is quite consistent from lab-to-lab, leading to good agreement in test results if the fans are well-behaved. If the fans are not well-behaved, meaning there is a significant amount of swirl at the fan's outlet or the fan's vibration is excessive, lab-to-lab variation can be quite high.

During an analysis of the air performance data from a high swirl fan we were able to tease out from the test results a correlation between air performance and the ratio of the outlet area of the fan to the area of the test chamber. This correlation is well known, but the results appear correlated to fan to chamber area ratios at ratios much higher than had previously been accepted. Sound power data, of course, was strongly correlated to fan vibration. An interesting note is that the uncertainties published in the aforementioned standards do not take into account errors associated with fan outlet area or fan vibration.

The CFD portion of this work focuses on gaining insight into the above mentioned correlation between air performance and the ratio of the outlet area of the fan to the area of the test chamber.

To mimic the above tubeaxial fan experiments a subset of five cases are selected to cover a wide range of area ratios. Full description of preferred solver setup, post processing method and simulation quality metrics is provided. Relative comparison of experimental vs. CFD data is presented. Finally, conclusions about performance predictions are offered.

THE CURRENT STATE OF FAN TESTING

The current state of air performance fan testing can best be described by the contents by the two most prominent test standards in use today, ISO 5801: 2007 and AMCA 210-07. In their current versions both of these standards acknowledge the problem swirl causes when trying to measure air performance, but they have differing approaches to the solution.

When a pressure measurement location is in a duct downstream of a fan with swirl, ISO 5801:2007 mandates a flow straightener be placed between the outlet of the fan and the pressure measurement location (Clause 27.2). AMCA 210-07 takes the opposite approach by mandating that setups with pressure measurement in a duct are not suitable for fans with significant swirl (Section 5.1.2). **Both standards,** however, allow the test of a fan with significant swirl on an outlet chamber (outlet ducted or not) with **no straightener** at all between the fan and the chamber where fan static pressure is measured (ISO 5801:2007 Clause 31.1 and AMCA 210-07 Section 5.1.2). Both standards require that the cross sectional area of the chamber be at least sixteen times the area of an axial fan outlet or outlet duct (nine times for a centrifugal). It's this ratio of sixteen that's of interest in this study.

The current state of sound testing can best be described by ISO 13347–1:2004 through 13347-4:2004 and AMCA 300-14. Both standards acknowledge vibration's effect on sound measurement (sound *output* actually), but neither require vibration measurement nor a maximum vibration level of the test setup, although AMCA 300-14 inches toward a requirement by suggesting a maximum vibration level of BV-3 (see notes in Figures 1, 2 and 3).

AIR PERFORMANCE COMPARISON METHOD

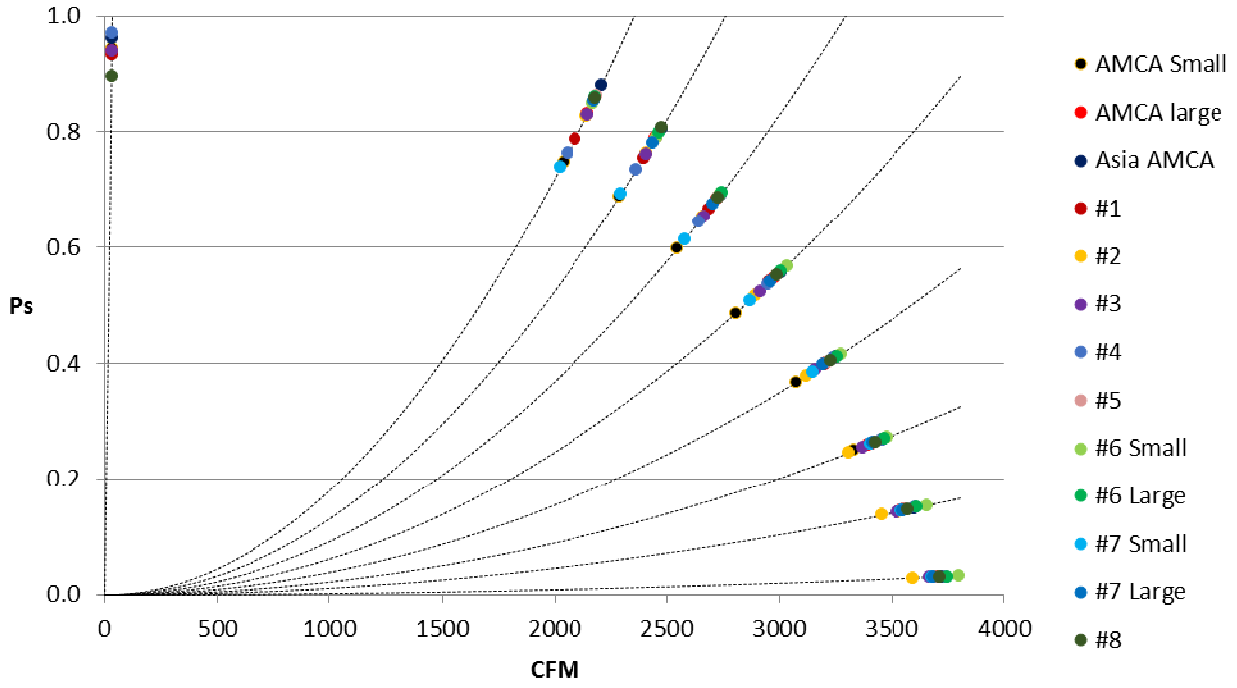

Figure 1: Typical fan curve / system curve intersection points

The basis of the air performance analysis was a comparison of air performance curves, or rather a comparison of discreet points on those curves. Because of the variation in test points and actual fan performance from lab-to-lab, it was necessary to first characterize each performance curve by a set of third order polynomials (or, moving polynomial), define parabolic system curves, then and use the intersections of each polynomial curve and system curve as points of comparison.

Comparisons of shaft power were done at identical percentages of wide open flow rate.

AIR PERFORMANCE COMPARISONS

The results of the round robin were as expected. Sans outliers, the curves of the vaneaxial and centrifugal fans were relatively tightly grouped, while the results of the tubeaxial were not as shown in Figures 2 and 3.

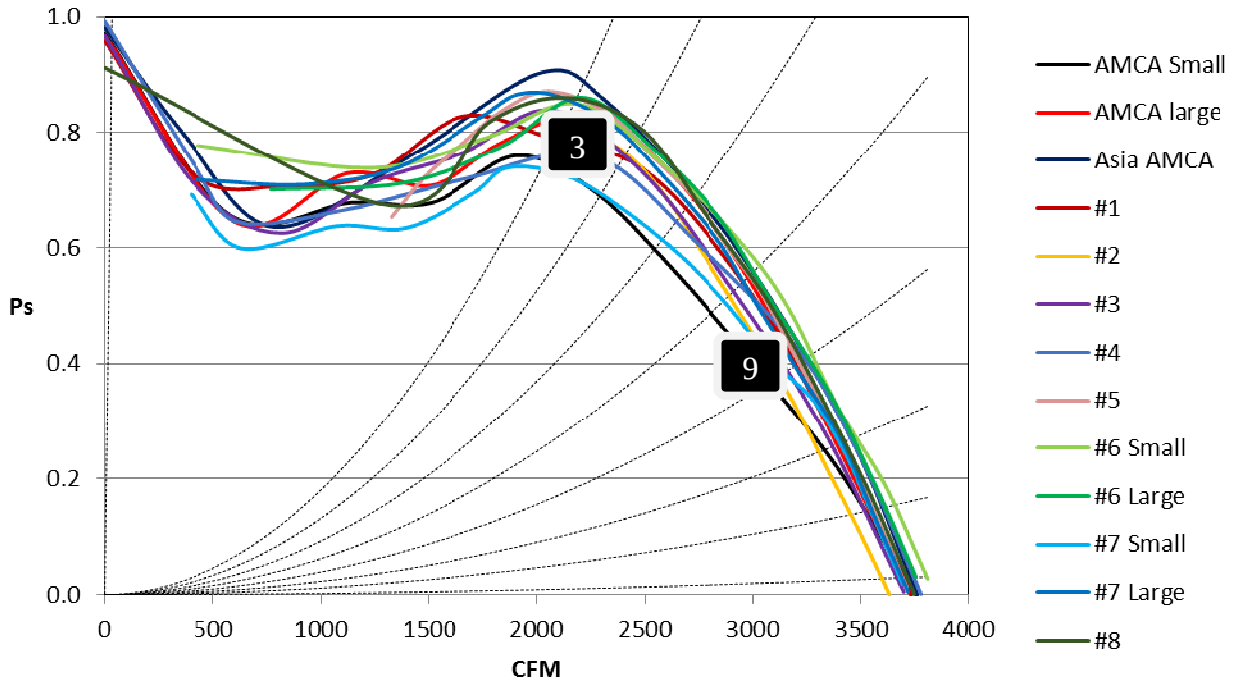

Figure 2: Plot of tubeaxial air performance results

The relative dispersal of the tubeaxial's test results can be seen in Figure 2, and is confirmed by the graphs below showing sample standard deviation divided by the mean at the system curve's intersection with each fan curve. Note the relatively high variation on power measurements of the vaneaxial given the relatively tight air performance measurement grouping. Recall that the vaneaxial power was determined with a calibrated power, with all labs using the same motor calibration.

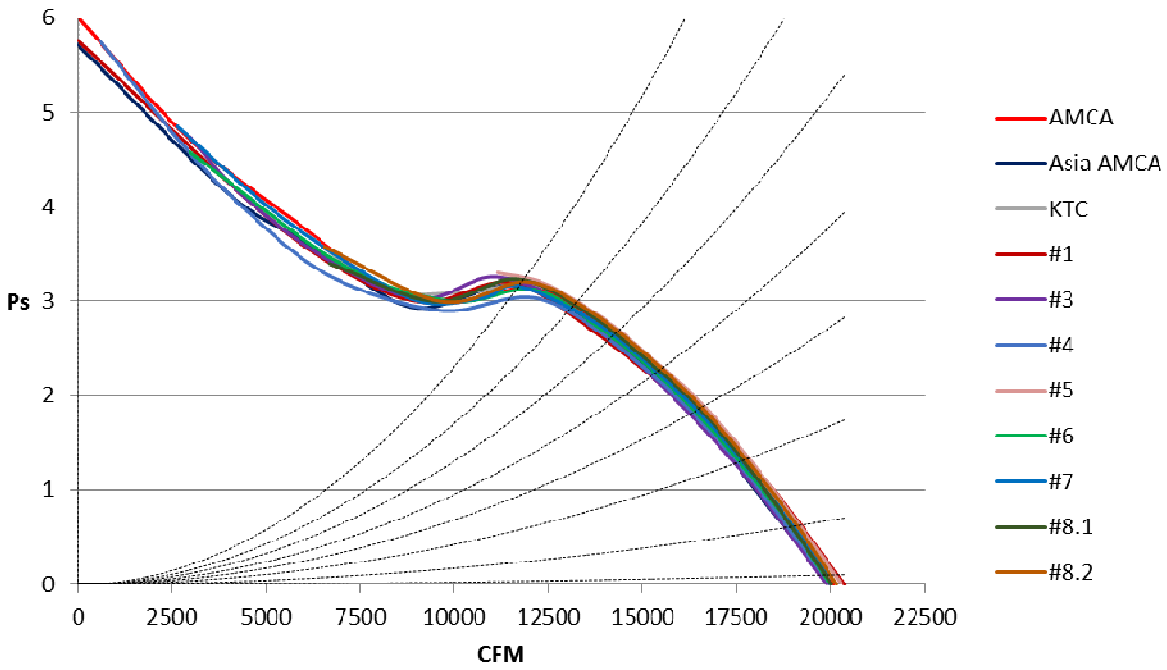

Figure 3: Plot of vaneaxial air performance results.
The grouping of the centrifugal results were similar to the vaneaxial.

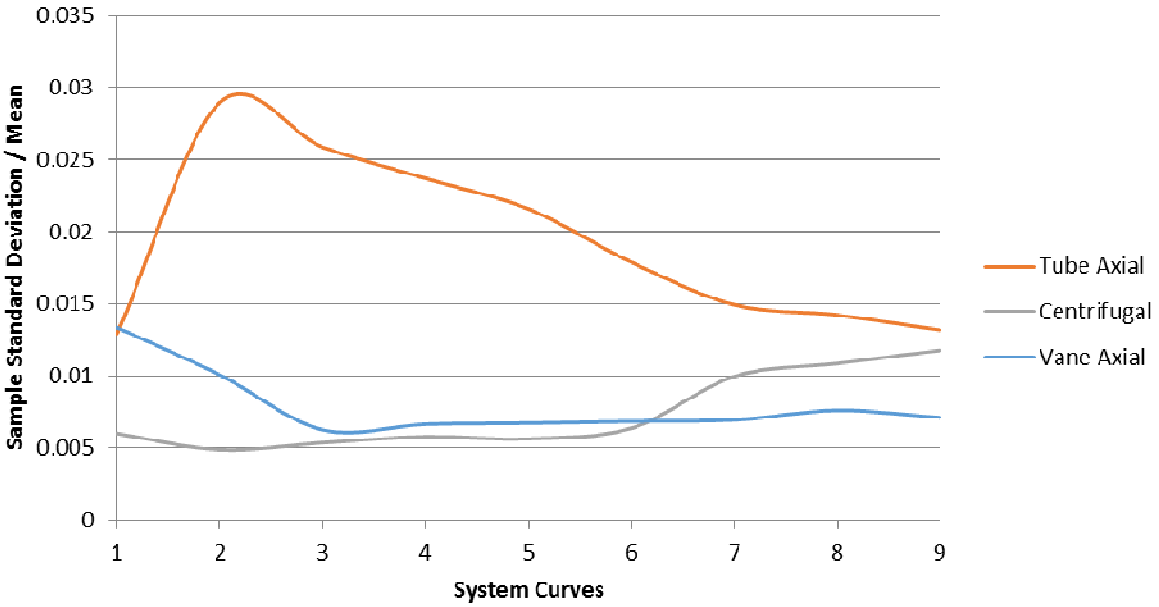

Figure 4: Flow rate measurement variation

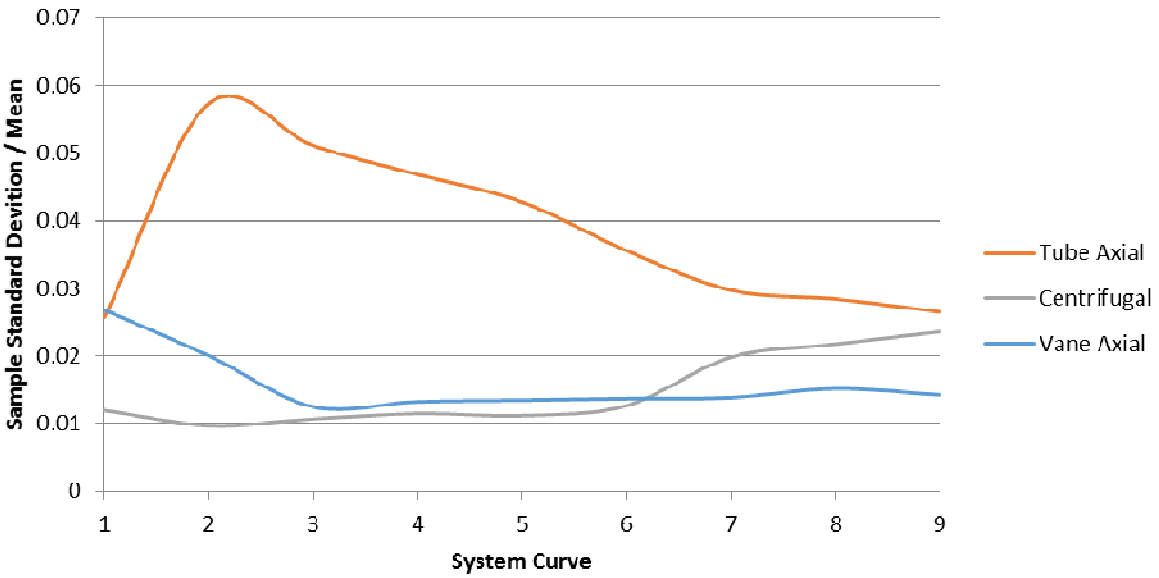

Figure 5: Static pressure measurement variation

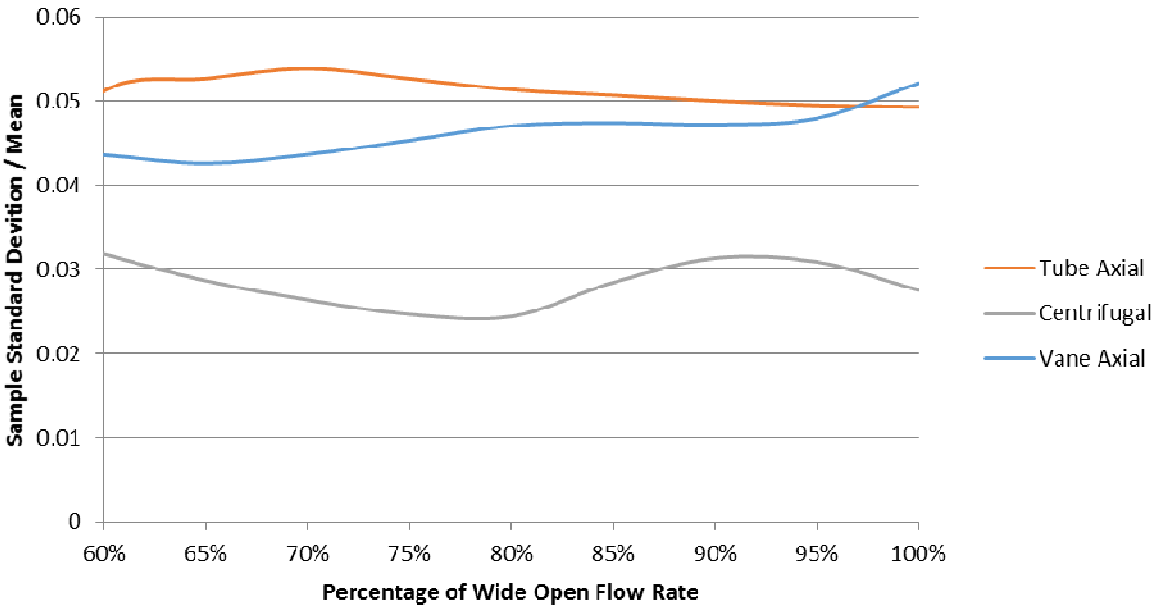

Figure 6: Shaft power measurement variation

Earlier investigation and experience pointed to the possibility that “small” ratios of chamber area to tubeaxial fan outlet area caused a systematic error in performance measurement. To investigate this further, we plotted fan static pressure against chamber/fan area ratio for each system curve. System curves three and nine are shown below. We chose to investigate static pressure rather than flow on the assumption that the settling screens upstream of the nozzle wall would remove any effect swirl imposed on flow measurement.

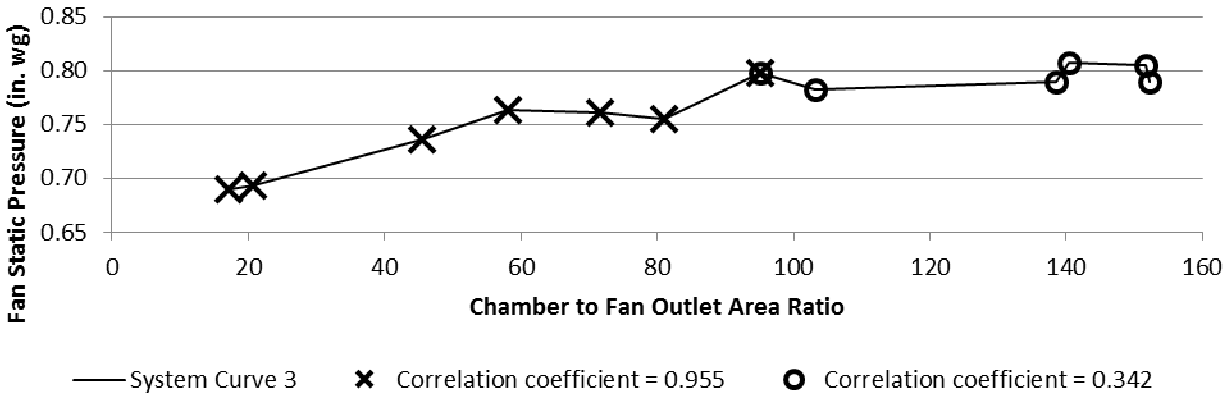

Figure 7: Fan static pressure versus chamber/fan area ratio for System Curve 3

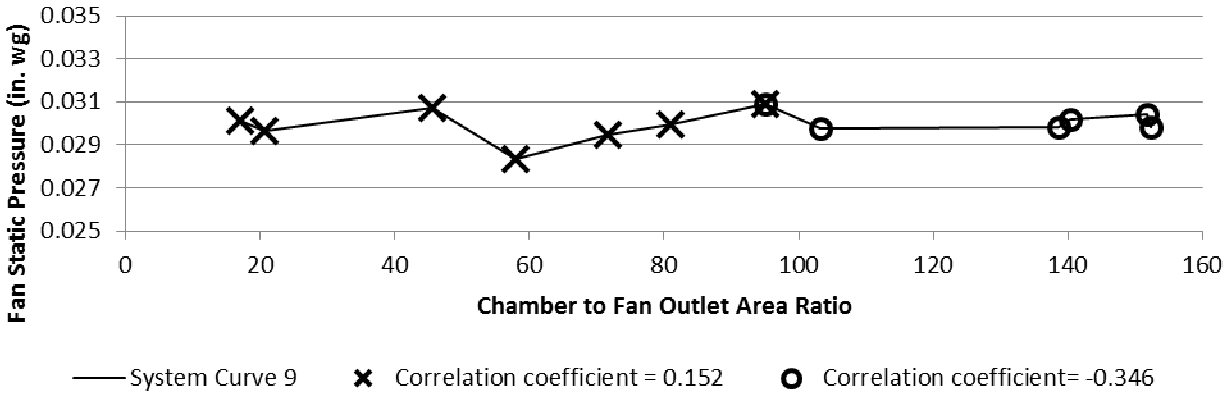

Figure 8: Fan static pressure versus chamber/fan area ratio for System Curve 9

There was no surprise in finding that measured fan static pressure measurement was higly correlated to chamber/fan area ratio, but what *was* surprising was the fact that this correlation persisted well above the ratio of sixteen, as would be expected from a reading of the test standards, and up to a ratio of approximately *ninety* near the best efficiency point. This correlation diminished signifantly as we moved down the static pressure curve toward free air.

SOUND MEASUREMENT COMPARISONS

Admittedly less effort went into this portion of the study, as severe vibration of the vaneaxial (which was driven by its own calibrated motor) attracted most of the attention in this area. But, this did capture the nessessity of both the ISO and AMCA versions of the sound test standard to pay more attention to fan vibration requirements, or maximum allowable vibration.

While Figure 9 shows lab-to-lab agreement within the check test tolerances of AMCA's Laboratory Accreditation Program, Figure 10 shows that a fan with high vibration makes this agreement impossible. In both plots, the check test tolerances were applied to the average L_w.

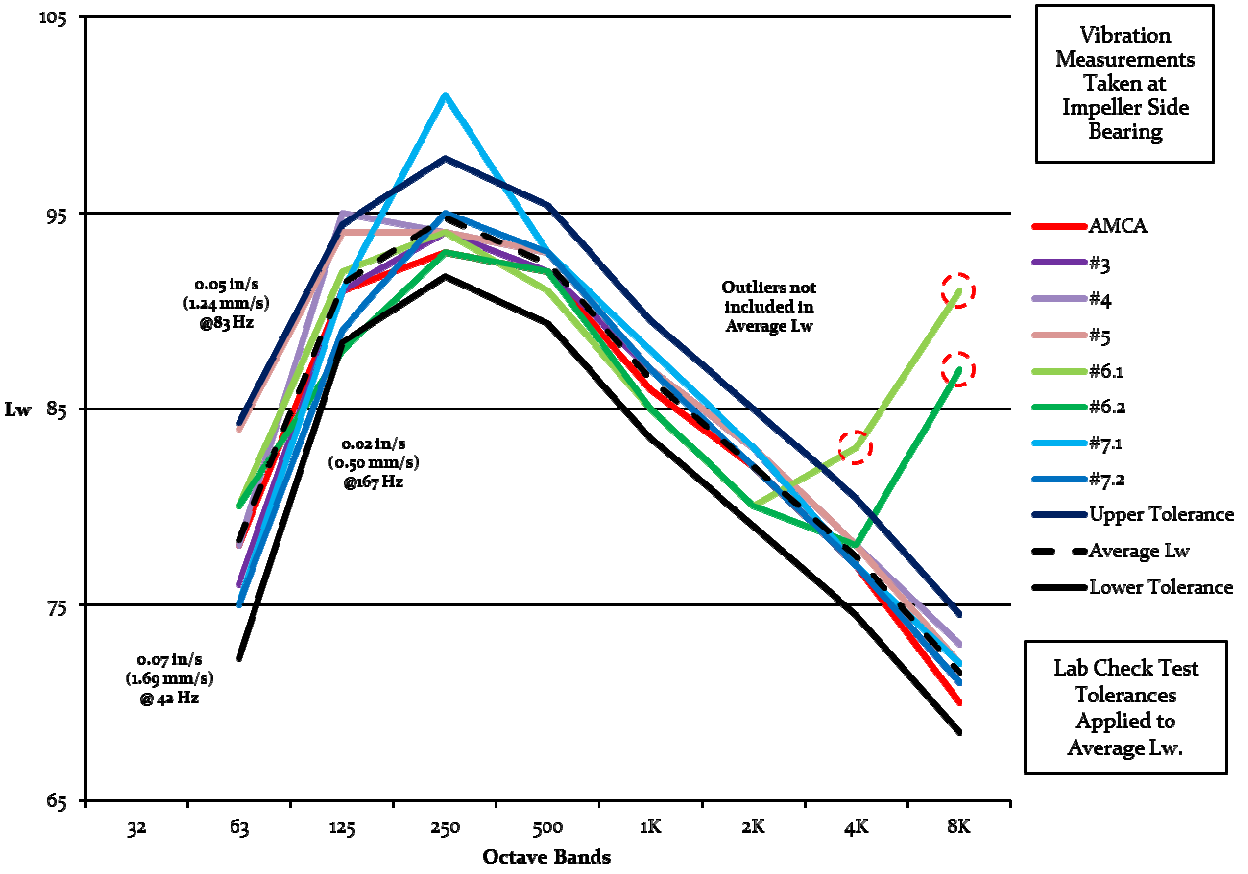

Figure 9: Tubeaxial sound power level spectrum

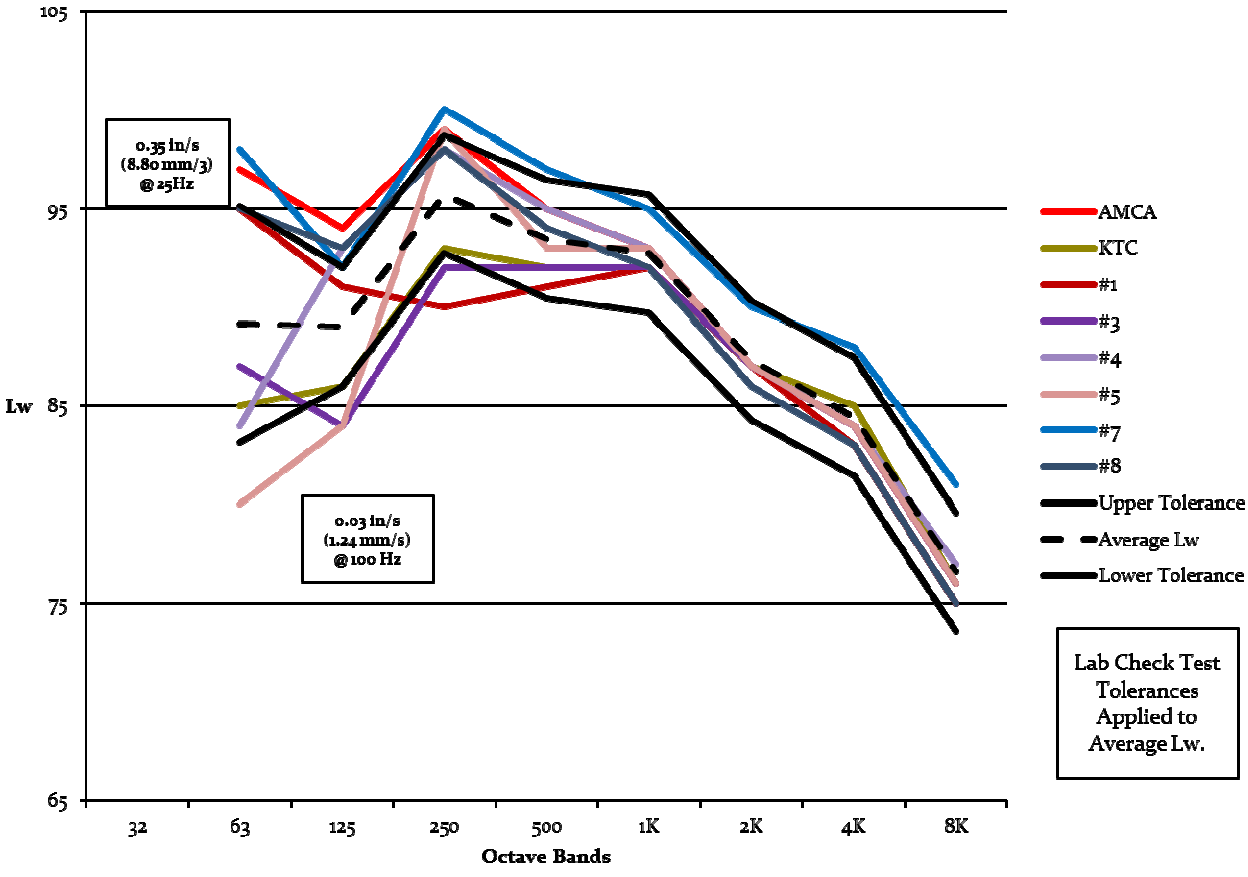

Figure 10: Vaneaxial sound power level spectrum

NUMERICAL FLOW SIMULATION

The computational fluid dynamics (CFD) portion of this work focuses on gaining insight into the above mentioned correlation between air performance and the ratio of the chamber to the fan outlet area. Of the thirteen fan curves that were compared in the study, Figure 11 shows the five fan curves with the chosen system curve that are to be reproduced using CFD.

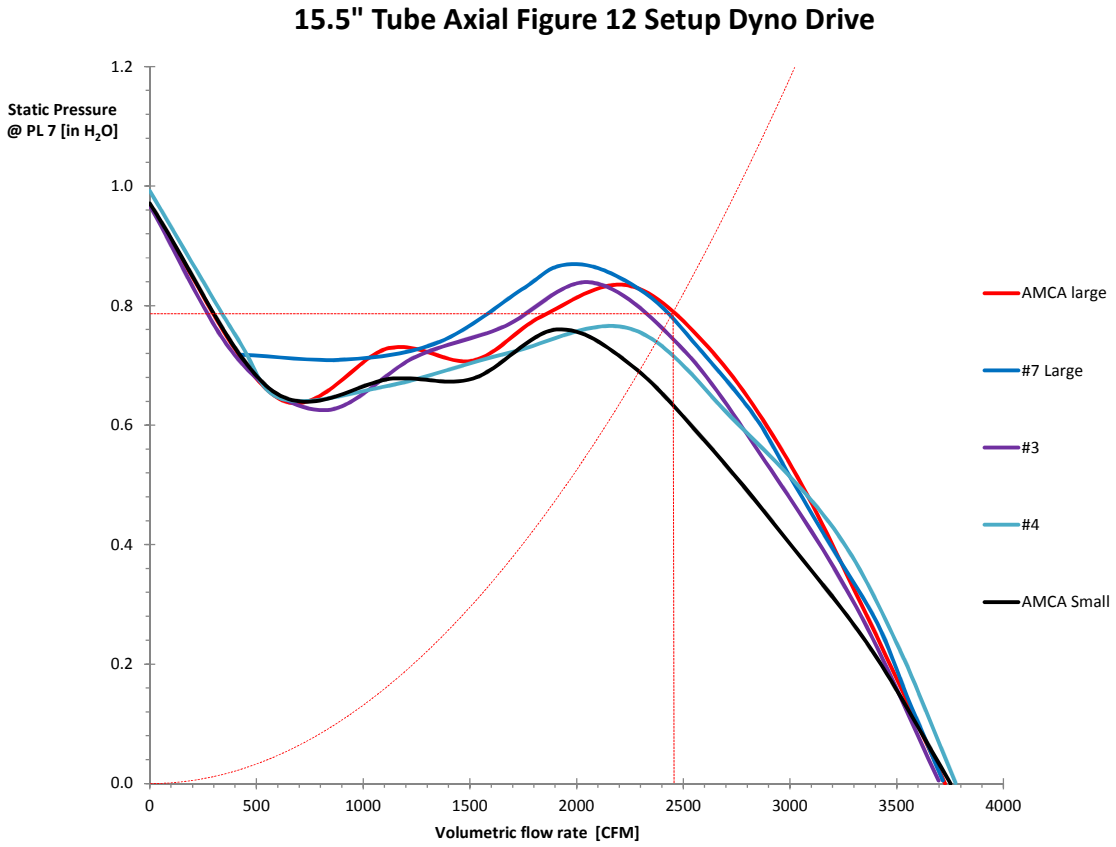

Figure 11: Subset of fan curves and the system curve chosen for CFD work

The subset of five curves is selected to cover a wide range of area ratios and two different chamber shapes. Table 1 shows the above data per chamber. Note that the smallest area ratio of the AMCA Small chamber is close to the ISO and AMCA recommended minimum area ratio of 16 [1].

Table 1: Chamber shape and area ratio information

Company	Chamber Shape	Chamber Area Ratio
AMCA Large	Rectangle	152.3
#7 Large	Rectangle	103.2
#3	Rectangle	71.6
#4	Round	45.6
AMCA Small	Round	17.0

The CFD model is based on a 15.5 inch diameter tubeaxial fan geometry with four generic, twisted blades mounted on the geometry in the CAD design space, see Figure 2. Ambient pressure at the inlet was modelled by a half-sphere, while the nozzle with a downstream pressure outlet was sized using the operating conditions of 2,500 cfm and 0.8 in.wg as shown in Figure 11 [2]. The chamber

model included a row of three settling means. Unstructured computational meshes were built with prism layers at all wall boundaries. The row of settling means was modelled by a series of porous jumps. Face permeability, porous medium thickness and the pressure-jump coefficient [7] were calibrated based on test data taken from both Greenheck's and AMCA's large chambers. The physical problem was defined as steady-state, isothermal and turbulent. An ANSYS Fluent pressure based solver was used in conjunction with the rotating reference frame (RRF) technique [7]. The K-ω shear stress transport (SST) turbulence model was employed to accurately capture adverse pressure gradients and flow separation.

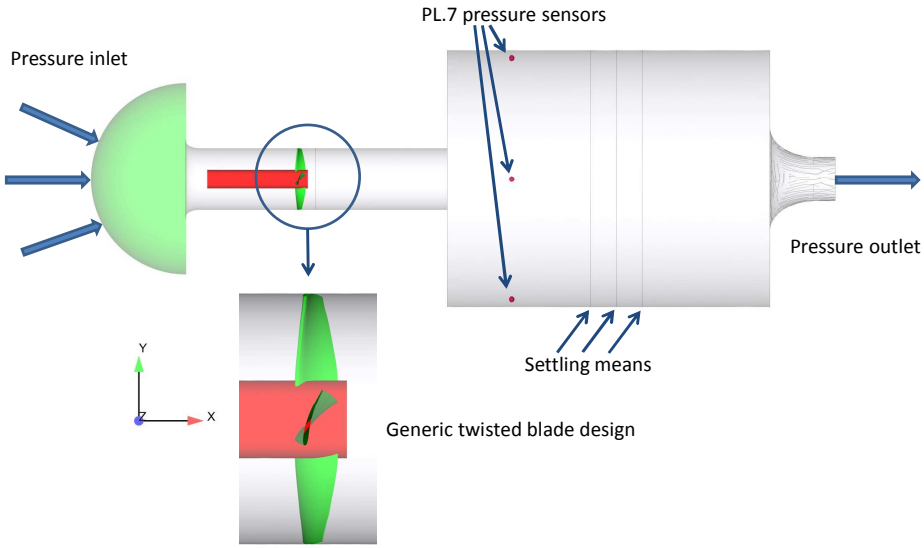

Figure 12: 15.5" generic tubeaxial and AMCA small outlet chamber CFD model

The initial CFD run was performed at a fan speed of 2500 rpm with ambient pressure applied at both the inlet and the outlet on the AMCA large chamber model. After this initial run converged, a custom written, fully parallelized user defined function (UDF) adjusted the fan's angular velocity to match the operating conditions picked under Figure 11. All subsequent runs use this adjusted fan speed of 2807 rpm for benchmarking purposes. Figure 13 depicts the AMCA Large chamber model at a fairly large volumetric flow rate as part of the calibration process. The high definition image captures the subsequent flow spread caused by the row of settling means within the chamber's front section [8].

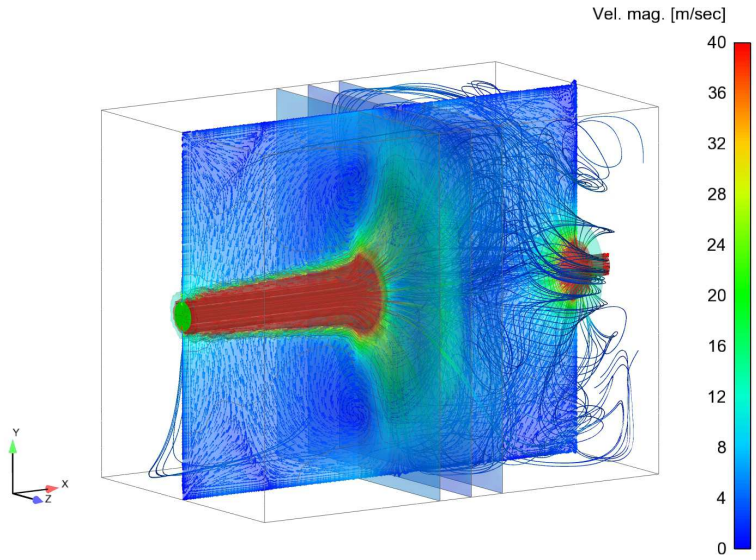

Figure 13: AMCA Large chamber – settling means calibration

COMPARISON OF RESULTS

Benchmarking the experimental data against the CFD results shows reasonable correlation as shown in Figure 14. Note that static pressure data is read via PL.7 sensors placed within all models per ISO and AMCA outlet chamber specifications in Figure 12.

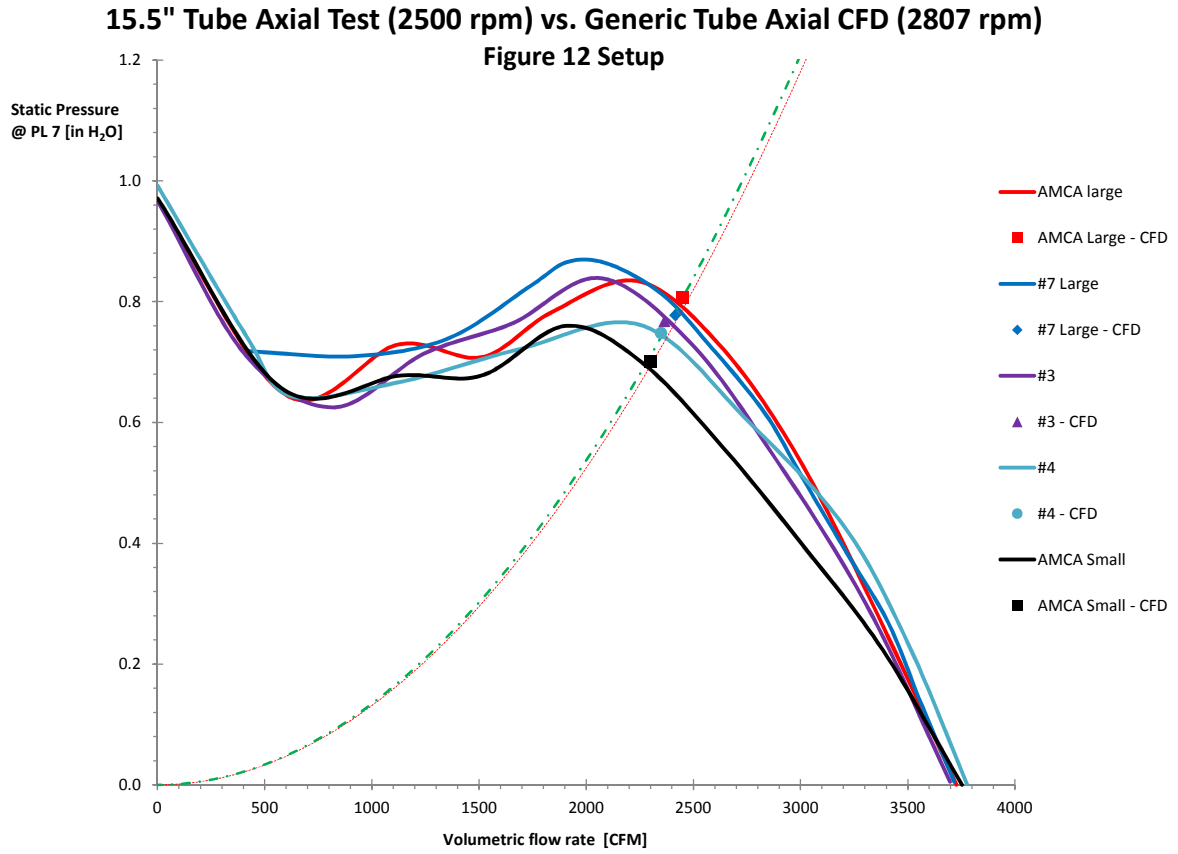

Figure 14: Benchmarking of experimental vs. CFD data

The following metrics are designed to compare swirling motion of the flow in the individual chamber front sections. This data also provides an insight into the scatter which is apparent from the performance data. Swirl is defined as a volume integral of x-vorticity in the chamber's front section. Similarly, tumble is defined as a vector sum of the volume integrals of y-vorticity and z-vorticity in the chamber's front section. Vorticity is defined as curl of the velocity vector:

$$\overline{\omega} = \nabla \times \overline{v} = \underbrace{\left(\frac{\partial w}{\partial y} - \frac{\partial v}{\partial z}\right)\underline{i}}_{\text{x-vorticity}} + \underbrace{\left(\frac{\partial u}{\partial z} - \frac{\partial w}{\partial x}\right)\underline{j}}_{\text{y-vorticity}} + \underbrace{\left(\frac{\partial v}{\partial x} - \frac{\partial u}{\partial y}\right)\underline{k}}_{\text{z-vorticity}}$$

Table 2 and Figure 15 show the calculated swirl and tumble vs. chamber area ratio results. It is apparent that the AMCA small chamber with the lowest chamber-to-fan area ratio produces an order of magnitude higher than average swirl and tumble numbers.

Table 2: Swirl and tumble results

Company	Chamber Area Ratio	Swirl [rpm]	Tumble [rpm]
AMCA Large	152.3	0.0026	0.189
#7 Large	103.2	0.0005	0.028
#3	71.6	0.0001	0.016
#4	45.6	0.0027	0.157
AMCA Small	17.0	0.0127	1.895

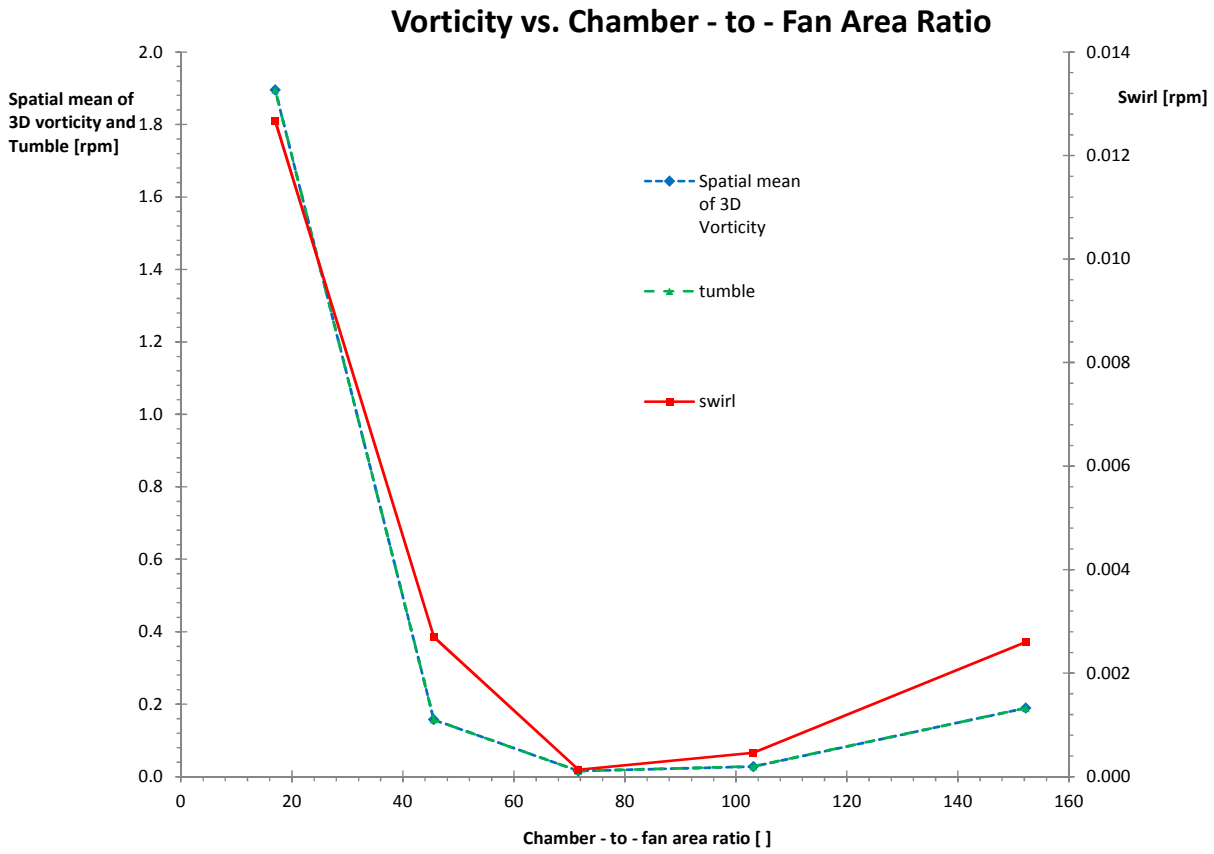

Figure 15: Vorticity vs. chamber area ratio results

Visual comparison of the two extreme chamber-to-fan area ratio models is shown in Figures 16 and 17. The same number of seeding points is defined at the pressure inlet to generate the visualization stream lines [8]. Although stream line density is not an accurate mean of flow representation it provides adequate visual information for general vorticity assessment. Both the streamline representation and the underlying velocity magnitude contour plots conclude that chambers with low area ratios fail to attain pressure recovery at the PL.7 pressure tap locations.

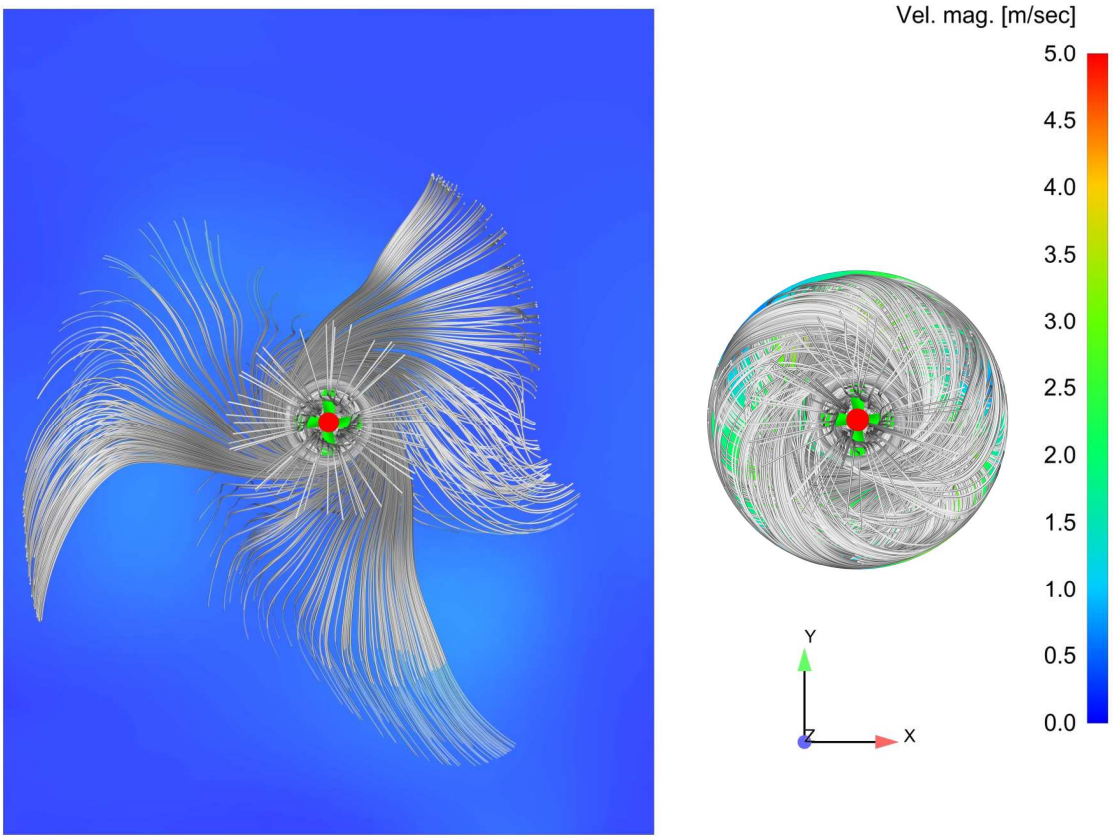

Figure 16: a) AMCA Large chamber vorticity - front view b) AMCA Small chamber vorticity – front view

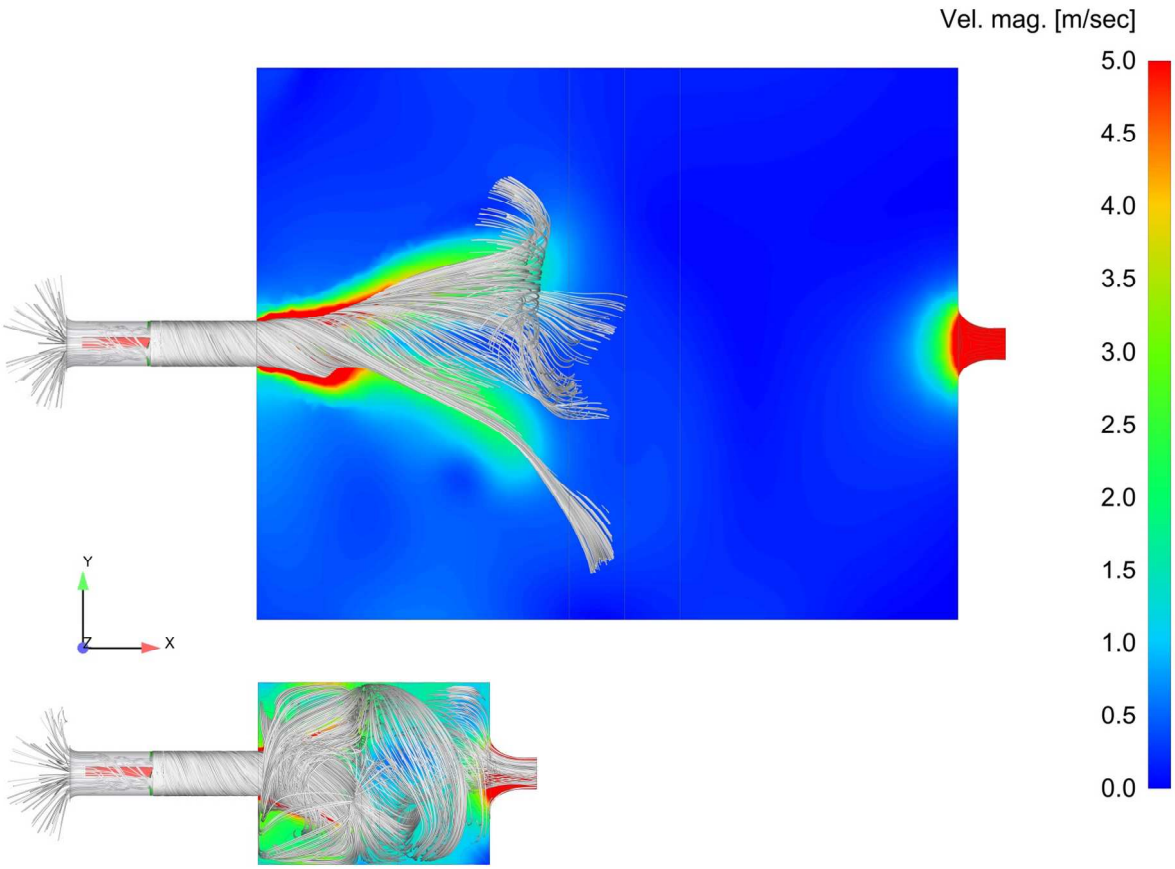

Figure 17: Side view of AMCA Large chamber vorticity (top) and AMCA Small chamber vorticity (bottom)

CONCLUSIONS

This paper concludes with recommended further study and changes to existing ISO and AMCA standards.

1. Both ISO 5801 and AMCA 210 should contain recommendations that high swirl fans be tested on an *inlet* chamber
2. If testing a high swirl fan on the inlet is not possible in all situations, increase the minimum area ratio for outlet chamber tests to a much larger ratio than sixteen. An international consensus would have to be reached on what that ratio should be, because some labs will have difficulty adapting for spatial and monetary reasons.
3. Both ISO 13347 and AMCA 300 should contain a mandatory measurement of fan vibration prior to the fan test and contain an admonition that the sound test *shall* not be run if a vibration level of BV-3 is not achieved by trim balancing. The current version of AMCA 300 does not stipulate a vibration measurement, and contains only a recommendation regarding whether or not the fan test may proceed if the vibration is greater than BV-3.
4. Further investigation into the effect of chamber shape, i.e. round versus rectangular, on swirl.
5. Further investigation into tests of both centrifugal and vaneaxial fans (fans without significant swirl) ducted into a chamber, and to whether or not the current area ratios for these fans are actually too stringent

BIBLIOGRAPHY

[1] ISO 5801 – *Performance testing using standardized airways.* **2007**

[2] ANSI/AMCA Standard 210. *Laboratory Methods of Testing Fans for Certified Aerodynamic Performance Rating.* **2007**

[3] Potter, A. C. and K. W. Burkhardt, *Test Chambers for Fans: Results of Tests Conducted by AMCA 210/ASHRAE 51 Committee.* **1975**

[4] ISO 13347–1–4, *Industrial fans — determination of fan sound power levels under standardized laboratory conditions.* **2004**

[5] ANSI/AMCA Standard 300. *Reverberant Room Methods for Sound Testing of Fans.* **2014.**

[6] ANSI/AMCA Standard 204, *Balance Quality and Vibration Levels for Fans.* **2012.**

[7] ANSYS. *Fluent User Guide*. Version 15.0. **2013**

[8] Computational Engineering International. *EnSight User Manual*. Version 10. **2014**

[9] Stevens, Mark. C631/034/2004. “Industrial fans — performance testing using standardized airways.” *International Conference on Fans.* **2004**